Proceedings of the 48th National Conference on Fluid Mechanics and Fluid Power (FMFP)
December 27-29, 2021, BITS Pilani, Pilani Campus, RJ, India.

FMFP2021–08–041

CFD Analysis of Secondary Flow and Particle transportation in Human Lungs

Ishita Jain[1], S.Sarkar[1]

[1]Department of Mechanical Engineering, IIT Kanpur, Kanpur-208016, India

ABSTRACT

The secondary flow characteristics and the deposition of inhaled pollutants across the bifurcation ridge have been simulated using a control volume method for a three dimensional laminar inspiratory flow. For the present simulation, lower three generation human lung-airway from fifth to seventh branches is extracted following the Weibel's model [1]. The extracted geometry is altered to create obstructions in order to study both symmetric and asymmetric form of Chronic Obstructive Pulmonary Disease (COPD). Computations are carried out for different particle diameters and number concentrations at Reynolds number (*Re*) of 1000 to replicate, understand and compare the physics of secondary flow in healthy and Asthma/ (COPD) affected human lung airway. Changes occurring in the the symmetric nature of secondary flow field, along and across the bifurcation ridge, arising due to various obstructions are profound. Mass flow rate imbalance, accumulation and newly generated vortices due to obstructions can be attributed to these changes.Further, the evolution of secondary vortices changes significantly due to inhaled pollutants where their deposition across the airways depends on their size and concentration.

Keywords: Particle Diameter, Particle Number Concentration, Secondary Flow, Vorticity.

1. INTRODUCTION

The flow dynamics in a human lung airway has been an important area of study since the 1960s right after the development of the simplest human lung model by Weibel [1]. With the increase in lung and nasal cancer risks caused by inhalation of various harmful particles, knowledge of such flow fields has become essential for understanding and perhaps controlling the causation of certain diseases like Asthma, chronic obstructive pulmonary disease (COPD), Interstitial Lung Disease (ILD), pneumonia, tuberculosis (TB). The enhanced respiratory problems faced in the present time are because of the imbalance imposed by urbanisations [1]. Major factors that lead to the augmentation of particle number in atmosphere are traffic and biomass burning. The pollutants dominating in an area depend upon their source and may differ with respective to their size, shape and concentration. Thorough understanding of such flow fields is also beneficial for targeted drug delivery, particulate inhalation, delivering therapeutic agents to the human body through inhalation. These therapeutic procedures have been widely accepted as a convenient, reproducible, and non-invasive method of drug delivery to the lung tissue and systemic circulation.

Until now numerous studies have been carried out, but they have been limited to either particle dosimetry [2] or flows in upper generation airways [3]. Some recent researches were dedicated to the computational study of the respiratory airflow characteristics in normal and obstructed human airways, but it was limited to primary flows and pressure depreciation [4,5]. Some experiments have also been carried out but have been limited to planar models. Zhao et al. [6] in their experiment on the flow in a single symmetric bifurcation using Laser Doppler Velocimetry (LDV) techniques for an inspiratory flow reported the presence of Dean vortices (two circular vortices of opposite sense).

Now with advancements like MRIs and CT scans it has become facile to obtain upper lung airway models but to understand physics of flow in lower airways researchers still like to depend on Weibel's [1] model. The present study aims to acquire and relate changes in secondary flow fields in the lower generation of human lung airway (generation 5 to 7) which is likely to be affected in cases of Asthma/COPD (for both symmetrical and asymmetrical domain). The study focuses on changes occurring in the flow field as flow progresses downstream at a Reynolds number 1000 corresponding to higher breathing rate to simulate conditions of Asthma/COPD. A 90º off plane configuration has been selected for its complexity and tortuous flow characteristics. Dean vortices along with anti-Dean vortices (four sets of vortices with pair of opposite rotating sense) are observed in Asthma affected human lung airway, whereas only Dean vortices (a pair of clockwise and anti-clockwise vortices at the cross section) were seen in the healthy case. The switchover from clockwise to anticlockwise vortices across bifurcation ridge is maintained irrespective of obstructions. Strength of the iso-surface vortex cores depends on the Reynolds number.

Also, the present study is an effort towards the global solution through understanding the evolution of vortices inside the airways apart from advection of aerosols carrying drugs. The effects of particle size and concentration on their transport and deposition in the respiratory tracts are studied. The changes in secondary flow fields in the lower generation of human lung airway (i.e., G5-G7), which is likely to be affected in the presence of pollutants, are analyzed.

S. Bhattacharyya and H. Chattopadhyay (eds.), *Fluid Mechanics and Fluid Power (Vol. 1)*,
Lecture Notes in Mechanical Engineering, https://doi.org/10.1007/978-981-19-7055-9_31

2. METHODOLOGY

2.1 Computational domain

A three-dimensional 90º off plane configuration, branching network is generated following the method of model geometry by Zhao et al. [6] and Liu et al. [7]. It comprises of three generations (namely generation 5 to 7) and are characterized by gradually decreasing diameters (from 3.5 mm in the first generation to 2.3 mm in the last generation) with 70º angle of bifurcation. To imitate Asthma/COPD, obstructions are constructed in the existing geometry in such a manner that the maximum depth, *d* is 0.5 mm and the radius of curvature, R is 2.32 mm from the outer wall. A schematic view of Asthma/COPD (asymmetrically obstructed) human lung geometry is shown in Fig. 1. The grid generation is achieved using ANSYS 15, where an unstructured mesh with sufficiently large number of tetrahedral elements (approximately 5.7 million) is used. A refined body fitted O-grid is used near the solid walls of the bronchial tubes to capture near wall gradients accurately.

2.2 Numerical details

The three-dimensional, steady, laminar incompressible viscous flows are used in the present study. The following continuity and momentum equations are solved numerically by finite volume technique using a commercial CFD package FLUENT 15,

$$\frac{\partial(\rho u_i)}{\partial x_i} = 0 \tag{1}$$

$$\frac{\partial(\rho u_i u_j)}{\partial x_i} = \frac{\partial P}{\partial x_j} + \mu \frac{\partial}{\partial x_i}\left(\frac{\partial u_j}{\partial x_i}\right) \tag{2}$$

The governing equation that describes particle motion is mentioned below:

$$\frac{\partial u_p}{\partial t} = F_D(u - u_p) + \frac{g_x(\rho_p - \rho)}{\rho_p}$$

where u and u_p are termed as fluid and particle velocity respectively. Here, only drag force is taken into consideration, which is denoted by F_D and is defined as:

$$F_D = \frac{18\mu}{\rho_p d_p^2}\frac{C_D Re_r}{24}$$

Where, Re_r is relative Reynolds number and is expressed as:

$$Re_r = \frac{\rho d_p |u_p - u|}{\mu}$$

The drag coefficient, C_D is obtained using the following formula:

$$C_D = a_1 + \frac{a_2}{Re_r} + \frac{a_3}{Re_r^2}$$

Where $a_1, a_2,$ and a_3 coefficients are determined for smooth spherical particles over several ranges of Re , given by [25].

For the present computational study, pressure-based SIMPLE algorithm is used to couple the velocity and pressure for solving the governing equations. The diffusion terms are discretized using a central difference scheme, while a second-order upwind scheme is used to discretize the advection terms in the unstructured three-dimensional mesh to reduce the numerical diffusion. To ensure fast convergence, a segregated implicit approach is used to obtain the steady solution. The two conditions are considered here differing in terms of total particle number concentration and particle size. The concentrations: one being negligibly polluted with almost clean flow representative of the countryside (C) and other case represent the urban site with 22,000 (U) particles introduced into the airways at the inlet. The sizes of particulate matter, which are imposed uniformly at the inlet, are 2, 5 and 10 μm under the assumptions that the particles are non-interactive and spherical. A uniform velocity inlet boundary condition has been applied to the branching network with no secondary velocity at the inlet. The gauge static pressure at the outlets is set to zero and the wall is provided with no-slip boundary condition in the present set of simulations. The Secondary velocity and vorticity are calculated following Guha et al. [3].

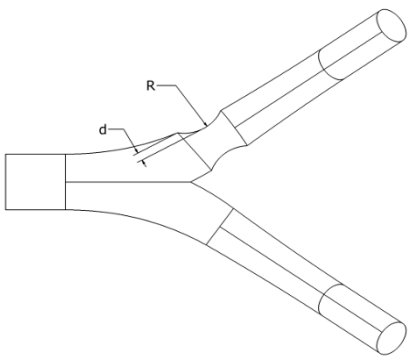

Figure 1: Schematic of Asthma affected (asymmetric) human lung airway with d = 0.5mm and R = 2.32mm, where d is the maximum depth and R is the radius of curvature of the upper cut.

Validation of results

The results obtained by present simulations for axial velocity at the end sections of generation 6 are compared with that of experimental results performed by Zhao et al. [6] at *Re* = 500. The numerical results also match well with Liu et al. [7].

3. RESULTS AND DISCUSSION

The secondary flow in the lower generation branches in a two-generation network with a single bifurcation module shows features similar to that in a curved pipe. In off plane geometry, the planes containing the centrelines of branches of a generation are rotated through 90° with respect to the plane containing the centrelines of their mother and grandmother branches, and hence complexities are associated with such a tortuous flow. The present study investigates the changes in the secondary flow field as the flow progresses downstream through different branching geometries. Obstructions are created by varying the cross section in generation 6 in order to estimate the secondary flow field in Asthma/ (COPD) affected human lung airways. λ_2 is the second largest eigenvalue of the symmetric tensor , where S and are the symmetric and anti-symmetric components of the velocity gradient tensor .

The changes in the secondary flow field across bifurcation modules and along curved portions are illustrated at different cross-sections through vector plots and streamwise vorticity. λ_2 criterion has been used to locate the vortex cores. λ_2 is the second largest eigenvalue of the symmetric tensor $S^2+\Omega^2$, where S and Ω are the symmetric and anti-symmetric components of the velocity gradient tensor. Figure 2 shows streamwise vorticity contours at sections of starting and end planes as flow passes through curved section of generation 6 (G06) at *Re* = 1000 for Asthma affected (asymmetric) human lung airway. The contours of streamwise vorticity are superposed with streamtraces.Branches with obstructions show different results from that of healthy lung airway like formation of Dean and anti-Dean vortices in the end planes of G06 and an increase in non-uniformity of secondary flow across end section (b) as shown. These changes can be attributed to the following reasons: (i) mass flow rate imbalance across bifurcation ridge, (ii) vortices created at the end of generation 6 because of the obstruction, (iii) changes in secondary flow in curved section of generation 6.

Figure 3 and 4 shows contours of secondary velocity and streamwise vorticity (superposed with secondary velocity vectors) at the end sections of generation 7 (G07). Vortices seem to rotate through 90º as the flow progresses through second bifurcation module. Moreover the line of symmetry also changes through 90º in generation 7. These changes can be attributed to the aforementioned reasons along with alterations created by second bifurcation. There are significant differences in flow structures of healthy and an Asthma affected human lung airway. In case of healthy lung airway, three vortex cores are observed, whereas the COPD affected airway develops initially a ring kind of structure after obstruction, which develops spiral vortex structure in G07 after bifurcation.

To appreciate the repercussions of inhaled pollutants, the changes in vorticity after injection of particles are presented in Figure 5 for the case U_1. The multiple numbers of vortex core with a complete loss of symmetry are observed as the flow passes through the bifurcating airways. Further, locations of particles in G07 for healthy airways are depicted in Figure 7 to get a detailed insight. The overall particle deposition increases with particle size, however distributions may not be symmetric in corresponding branches. The trapped particles are preferentially accumulated in the upper airways and near carinal ridge as shown in the Table 1 by estimating deposition efficiency on the upper and lower generation walls.

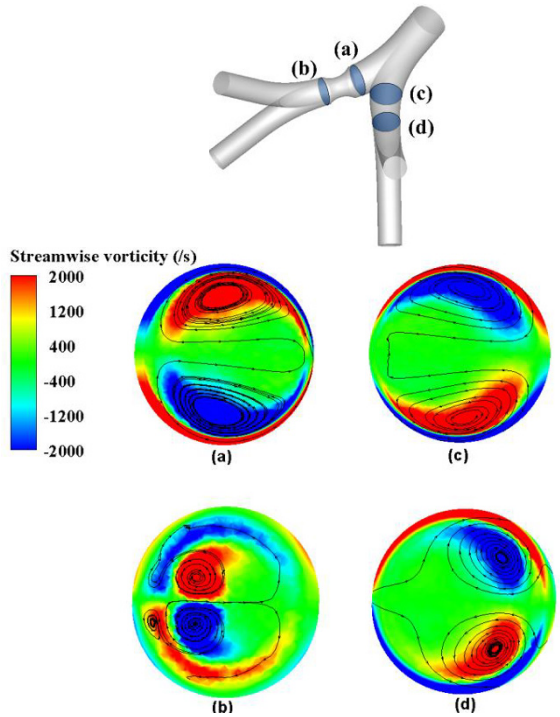

Figure 2: Streamwise vorticity contours superposed with streamtraces at the end planes of branches of G06 at *Re* =1000 of an Asthma affected human lung airway.

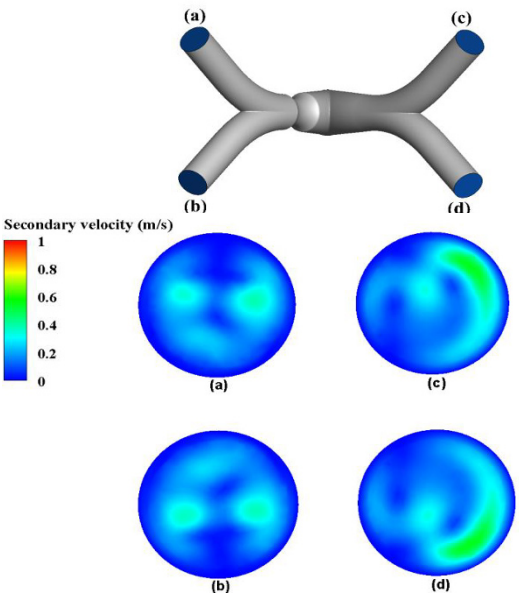

Figure 3: Secondary velocity contours at the end planes of branches of G07 at *Re* = 1000 of an Asthma (asymmetric) affected human lung airway.

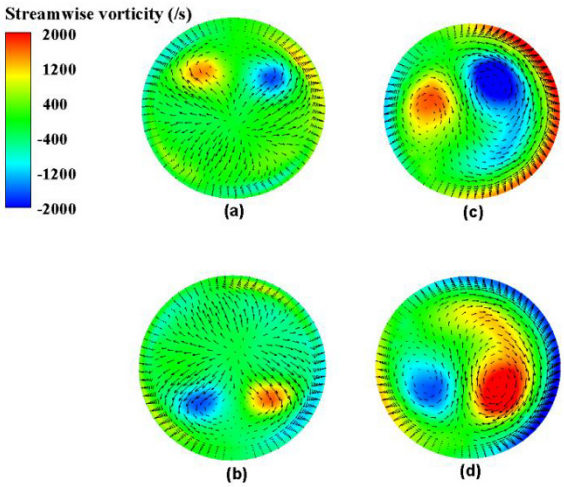

Figure 4: Streamwise vorticity contours superposed with secondary velocity vectors at the end planes of branches of G07 at *Re* =1000 of an Asthma (asymmetric) affected human lung airway.

\

Figure 5. Locations of particles in airway with 2μm diameter for the case U_1.

Table 1: Deposition efficiency of particles in airways for the case U_1 at upper wall (carinal ridge) and branches of G07 generation

Particle Diameter (µm)	Deposition Efficiency (%)	
	Upper Wall (near carinal ridge)	*G07 Branches*
2 µm	24 %	7 %
5 µm	42 %	28 %
10 µm	54 %	40 %

4. CONCLUSIONS

The present study reveals the flow structures through the human lung airway for both healthy and Asthma affected lung. Enriched secondary flows are observed due to bifurcations of airways. Furthermore, the obstructions replicating the COPD/Asthma affected lung airway enhances the non-uniformity of secondary flows. The obstruction initially creates ring vortices that end up to spiral vortices after bifurcation. As the complexity of obstructions increases as in case of severe Asthma/COPD, symmetric nature across or along the bifurcation ridge vanishes with complex vortex cores. The particle deposition increases with particle size and the trapped particles are preferentially accumulated in the upper airways and near carinal ridge.

NOMENCLATURE

u	Fluid (air) velocity	[m/s]
u_p	Particle velocity	[m/s]
Re_r	Relative Reynolds number	--
g	Acceleration due to gravity	[m/s^2)]
ρ	Density of air	[kg/m^3]
ρ_p	Particle density	[kg/m^3]
C_D	Drag coefficient	--

REFERENCES

[1] Weibel, Ewald R. "Geometric and dimensional airway models of conductive, transitory and respiratory zones of the human lung." Morphometry of the human lung. Springer, Berlin, Heidelberg, 1963. 136-142.

[2] Hofmann, Werner. "Modelling inhaled particle deposition in the human lung—a review." Journal of Aerosol Science 42.10 (2011): 693-724.

[3] Guha, Abhijit, and Kaustav Pradhan. "Secondary motion in three-dimensional branching networks." Physics of Fluids 29.6 (2017): 063602.

[4] Sul, B., Wallqvist, A., Morris, M. J., Reifman, J., & Rakesh, V. (2014). A computational study of the respiratory airflow characteristics in normal and obstructed human airways. Computers in biology and medicine, 52, 130-143.

[5] Yang, X. L., Liu, Y., & Luo, H. Y. (2006). Respiratory flow in obstructed airways. Journal of biomechanics, 39(15), 2743-2751.

[6] Zhao, Yao, and Baruch B. Lieber. "Steady inspiratory flow in a model symmetric bifurcation." Journal of biomechanical engineering 116.4 (1994): 488-496.

[7] Liu, Y., R. M. C. So, and C. H. Zhang. "Modeling the bifurcating flow in a human lung airway." Journal of biomechanics 35.4 (2002): 465-47